Electrochimica Acta 192 (2016) 89–98

Contents lists available at ScienceDirect

Electrochimica Acta

journal homepage: www.elsevier.com/locate/electacta

Towards effective small scale microbial fuel cells for energy generation from urine

Jon Chouler[a,b], George A. Padgett[a], Petra J. Cameron[c], Kathrin Preuss[d,e], Maria-Magdalena Titirici[d,e], Ioannis Ieropoulos[f], Mirella Di Lorenzo[a,*]

[a] University of Bath, Department of Chemical Engineering, Bath BA2 7AY, UK
[b] Centre for Sustainable Chemical Technologies, University of Bath, Bath BA2 7AY, UK
[c] University of Bath, Department of Chemistry, Bath BA2 7AY, UK
[d] Queen Mary University of London, School of Engineering and Materials Science, London, E1 4NS, UK
[e] Queen Mary University of London, Materials Research Institute, London E1 4NS, UK
[f] Bristol BioEnergy Centre, Bristol Robotics Laboratory, University of the West of England, Bristol, UK

ARTICLE INFO

Article history:
Received 29 October 2015
Received in revised form 14 January 2016
Accepted 15 January 2016
Available online 18 January 2016

Keywords:
Microbial Fuel Cell
Urine
Biochar
Bioenergy

ABSTRACT

To resolve an increasing global demand in energy, a source of sustainable and environmentally friendly energy is needed. Microbial fuel cells (MFC) hold great potential as a sustainable and green bioenergy conversion technology that uses waste as the feedstock. This work pursues the development of an effective small-scale MFC for energy generation from urine. An innovative air-cathode miniature MFC was developed, and the effect of electrode length was investigated. Two different biomass derived catalysts were also studied. Doubling the electrode length resulted in the power density increasing by one order of magnitude (from 0.053 to 0.580 W m^{-3}). When three devices were electrically connected in parallel, the power output was over 10 times higher compared to individual units. The use of biomass-derived oxygen reduction reaction catalysts at the cathode increased the power density generated by the MFC up to 1.95 W m^{-3}, thus demonstrating the value of sustainable catalysts for cathodic reactions in MFCs.

1. Introduction

In the face of the growing problem of fossil fuel depletion, there is global interest in developing sustainable and environmentally friendly forms of energy. One form of alternative energy that may be viable in addressing this problem is bioenergy [1,2]. In this context, Microbial fuel cells (MFC) hold great potential as green and carbon-neutral technology that directly converts biomass into electricity [3].

MFCs are electrochemical devices that take advantage of the metabolic processes of microorganisms to directly convert organic matter into electricity with high efficiencies for long periods of time [4]. Compared to other bioenergy conversion processes (i.e. anaerobic digestion, gasification, fermentation), MFCs have the advantage of reduced amounts of sludge production [5], as well as cost-effective operation, since they operate under ambient environmental conditions (temperature, pressure) [6]. Moreover, MFCs require no energy input for aeration so long as the cathode is passively aerated, for example *via* the use of a single-chamber device [7]. Lastly, MFCs have the ability to generate energy remotely by using a range of feed stocks, and can thus be used in areas of poor energy infrastructure. Organic waste used as a feed stock in particular offers attractive prospects from its cost-effectiveness and abundance. Urine has been demonstrated to be an effective feed stock for MFC operation with the additional benefit of nitrogen, phosphate and potassium recovery from the fuel [8]. In particular, according to Ieropoulos et al [9]. urea is enzymatically hydrolysed to ammonia and carbon dioxide. Ammonia is then oxidised at the anode of the MFC to generate mainly nitrite and in smaller amounts nitrate [10].

Despite the breadth of applications and the growing interest in MFC technology over the past two decades, commercialisation of MFCs for energy generation has not yet been realised.

The major limiting factors that hinder the practical implementation of MFCs at large scale, are the cost of materials used and the difficulties in the scale-up process [11].

Typically the electrodes are made from highly cost-effective materials such as carbon cloth, carbon paper, and graphite based

* Corresponding author. Tel.: +44 1225 385574.
E-mail address: M.Di.Lorenzo@bath.ac.uk (M. Di Lorenzo).

http://dx.doi.org/10.1016/j.electacta.2016.01.112

rods, plates and granules. Recently, even some metals, such as copper and silver, have been shown to be effective anode materials [12]. However, expensive metals, such as platinum, are usually used at the cathode to enhance the oxygen reduction reaction (ORR) [13–15]. Recently, the use of biomass-derived catalysts recovered from waste has been proposed as an effective alternative to expensive metal ORR catalysts. In particular, biomass-derived materials from wood [16], sewage sludge [17] and bananas [18] have been shown to function as ORR catalysts to boost MFC performance whilst reducing the device cost and its carbon footprint. Doping these materials with heteroatoms such as nitrogen and sulphur [19], also in combination with nanoparticles like iron [20], has been shown to enhance the catalytic activity towards the ORR even further.

Another limitation towards practical implementations of MFCs, is their poor performance due to high internal resistances and ohmic losses experienced upon scale-up [21]. Consequently, the power performance of MFCs is low compared to other renewable energy technologies [8,22]. Considering the thermodynamic limit of an MFC (1.14 V open circuit), the most feasible approach to scale-up the power generated by this technology is to create a collection of multiple MFCs connected together as a stack. By miniaturising individual MFC units, stacks of large numbers of constituent MFCs could be developed, within a compact footprint. This approach has been referred as the 'miniaturisation and multiplication' strategy [9].

MFC miniaturisation offers other advantages as well. The large surface area-to-volume ratio and short electrode distances - typical characteristics of miniature MFCs- provide a pathway to reducing ohmic losses, improving the mass transport processes between bulk liquid, biofilm and electrode and therefore enhancing power performance [23]. The consolidation of microfabrication techniques has led to the first prototypes of micro-sized MFCs, which have been discussed in a recent review [11]. Nonetheless, the process of miniaturisation of the MFC technology is still in its infancy. The two-chamber configuration is typically adopted for the miniature MFCs reported thus far, and, usually, a ferricyanide solution is used as the catholyte [24]. Given the greater operational simplicity and cost-effectiveness of oxygen diffusion systems, air-cathode MFC designs should be considered instead. Moreover, a more in-depth analysis on how to effectively miniaturise the system for better performance would be beneficial.

With the aim of guiding the development of efficient small-scale MFCs, this study reports the development of an innovative air-cathode small-scale MFC and analyses the effect that the chamber length (and therefore the electrodes length) have on its performance either when operated as a single unit or when assembled in a stack. No expensive metals have been employed at the cathode, and the use of two types of innovative and highly sustainable biomass-derived ORR catalysts are compared with a catalyst-free device.

2. Experimental

2.1. Materials

All reagents used were of analytical grade and purchased from Sigma-Aldrich and Alfa Aesar. Unless otherwise stated, all aqueous

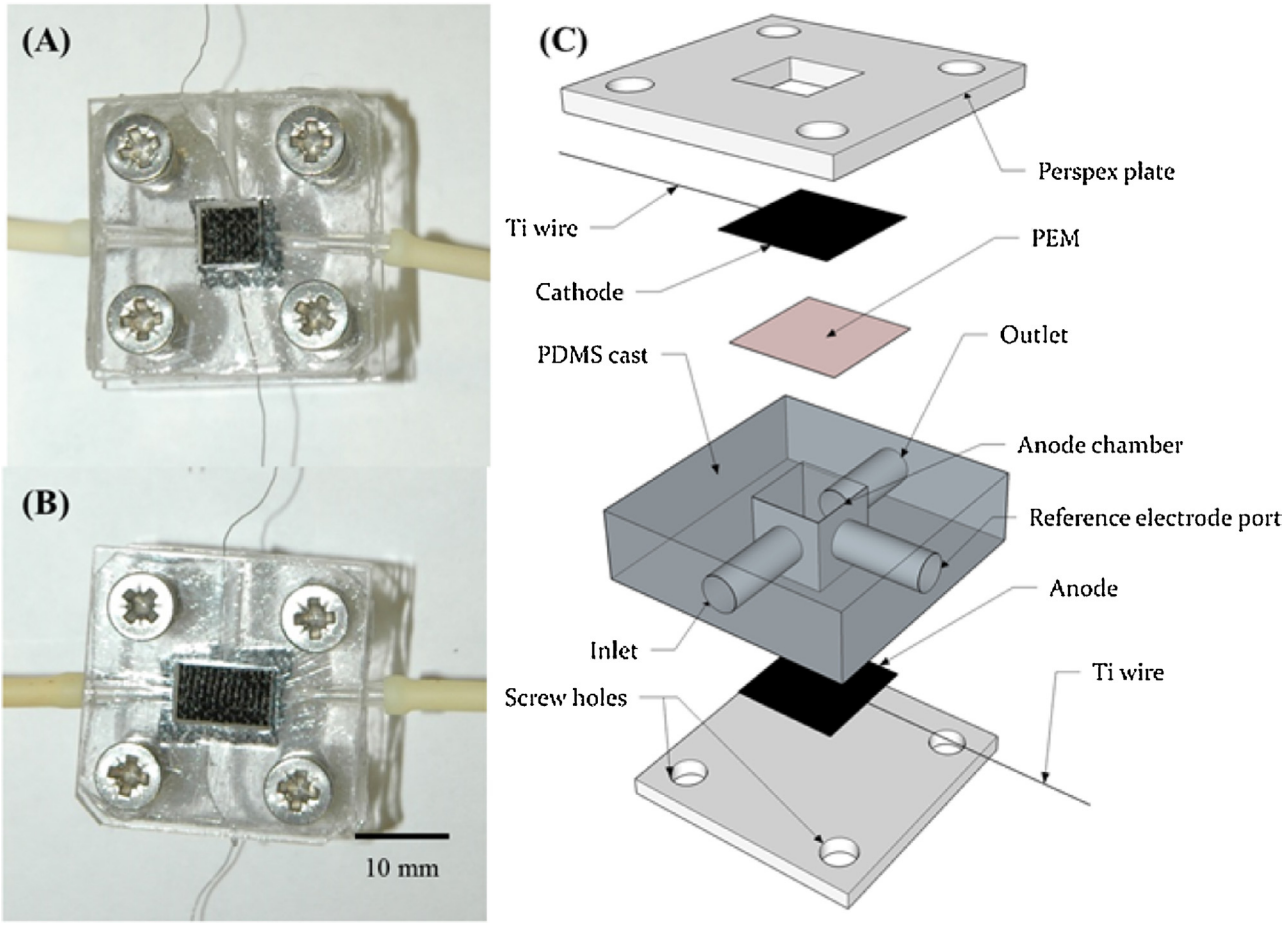

Fig. 1. MFCs used in this study; A: Photograph of MFC_S; B: Photograph of MFC_L; C: Schematic layout of the device.

solutions used were prepared with reverse osmosis purified water. Polydimethylsiloxane (PDMS, Dow Corning Sylgard 184) was purchased from Ellsworth Adhesives (UK).

Artificial Urine Medium (AUM) was used as the feedstock and prepared as previously described [25]. Tetrasodium pyrophosphate was added to the AUM as a precipitation inhibitor. The resulting feedstock was sterilised by filtration (Grade p8 filter paper, Fisher Scientific, UK) prior to use.

2.2. Microbial Fuel Cells

Two geometries were used in this study, leading to the fuel cells MFC_S (for short length) and MFC_L (for longer length). Both MFCs consisted of a single chamber made of a rectangular piece of PDMS and sandwiched between two Perspex plates (Fig. 1). The channel mould was made of PA 2200 nylon plastic and purchased from Shapeways, New York, USA. The top plate had a square opening as large as the channel cross sectional area to host the cathode, which was opened to air. The anode was instead placed at the bottom of the channel. The two geometries considered differed from each other according to the length of the anode chamber. In particular, MFC_S was characterised by a total anodic chamber volume of 64 μL (length = 4 mm, width = 4 mm, height = 4 mm), while MFC_L had an anodic volume of 128 μL (MFC_L: length = 8 mm, height = 4 mm, width = 4 mm).

The anode and cathode (geometric surface area = 16 mm^2 for the case of MFC_S, and 32 mm^2 for MFC_L) were made of carbon cloth (untreated carbon cloth type-B, E-Tek, USA) and threaded with titanium wire (Advent Research Materials, Oxford, UK) for electrical contact. The proton exchange membrane (Nafion® 115, Sigma-Aldrich) was hot pressed to the cathode by applying a pressure of approximately 2.5 bar for 12 minutes at a temperature of 150 °C.

2.3. Use of a biomass-derived oxygen reduction reaction catalyst

Two different biomass-derived ORR catalysts, named as BC1 and BC2, produced by hydrothermal carbonisation, were tested at the cathode of MFC_L. Both catalysts were synthesised from glucose and ovalbumin as described in [26] and [19]. BC1 is a nitrogen doped carbon aerogel, while BC2 is a nitrogen and sulphur co-doped aerogel that was prepared with an additional iron source. A loading of 1.5 mg per cm^2 of the cathode area was used for each ORR catalyst. 1.5 mg of catalyst was mixed with 105 μL of Nafion® perfluorinated resin solution and sonicated for 3 minutes. The resulting suspension was spread over 1 cm^2 of carbon cloth. Once dried, the doped cathode was bound to the Nafion® membrane as shown in Fig. 1 above. The MFCs with the doped cathodes were named as MFC_BC1 and MFC_BC2, according to the ORR catalyst used.

The morphology of the resulting electrodes was characterised using a Hitachi S-4300 scanning electron microscope (SEM).

2.4. Operation of the MFCs

All MFCs were fed with AUM at the flow rate of 0.36 mL min^{-1} (hydraulic residence times of 11 seconds and 22 seconds for MFC_S and MFC_L respectively). The cells were connected to a multi-channel peristaltic pump (Ecoline, Ismatech, Germany) *via* Pharmed® BPT tubing, ID 1.6 mm (Cole-Parmer, UK). The anode and cathode were connected to a voltmeter (ADC-24 Pico data logger, Pico Technology, UK) and to an external load to polarise the cell and monitor the cell potential under closed circuit conditions.

Maturing of the electrochemically active bacteria (enrichment) at the anode was performed over a period of five days. It consisted of feeding the MFCs under continuous recirculation conditions with AUM containing 1% *v/v* mixed culture of bacteria (anaerobic sludge provided by Wessex Water, Scientific Laboratory in Saltford, UK), which was replaced on a daily basis. The fuel cells were first

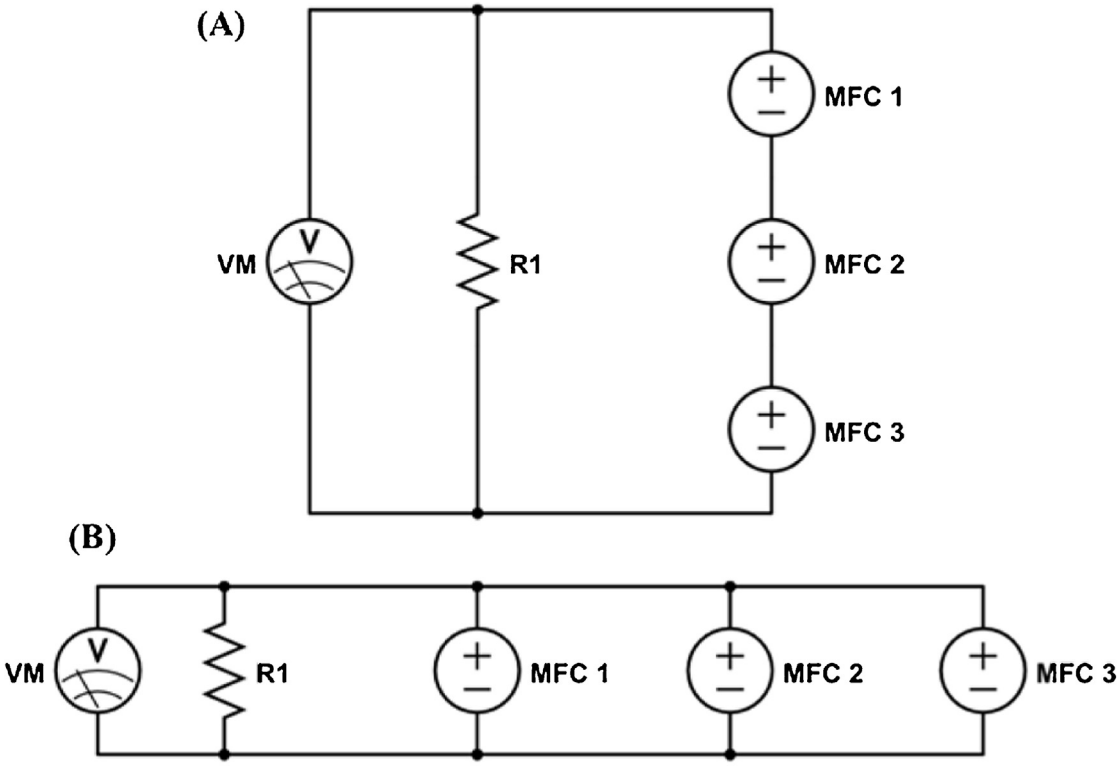

Fig. 2. Schematic for electrical stacking MFC units in series (A) and in parallel (B): R1 = external load, VM = voltmeter.

operated under open circuit conditions for up to 2 hours, and then connected to an external load of 1 kΩ. After the enrichment, the MFCs were fed continuously with AUM and no bacteria.

Polarisation experiments were performed by connecting the MFCs to a series of external loads, varying from 10 Ω to 1000 kΩ, controlled by an external variable resistor (RS-200 Resistance substitute, IET Labs Inc., USA), and by measuring the pseudo steady state output potential after 20 minutes. Before the test, the MFC was left under open circuit for no more than 2 hours to allow a steady state open circuit voltage (OCV) to develop. Ohm's law was used to determine the corresponding current (I) at each external load value ($I = V/R$, where V, and R are voltage and resistance respectively). The power (P) was calculated by using Joule's law ($P = I^2/R$). Power density was calculated by dividing the power by the MFC chamber volume, while current density was calculated by dividing the current by the total macro surface area of the anode.

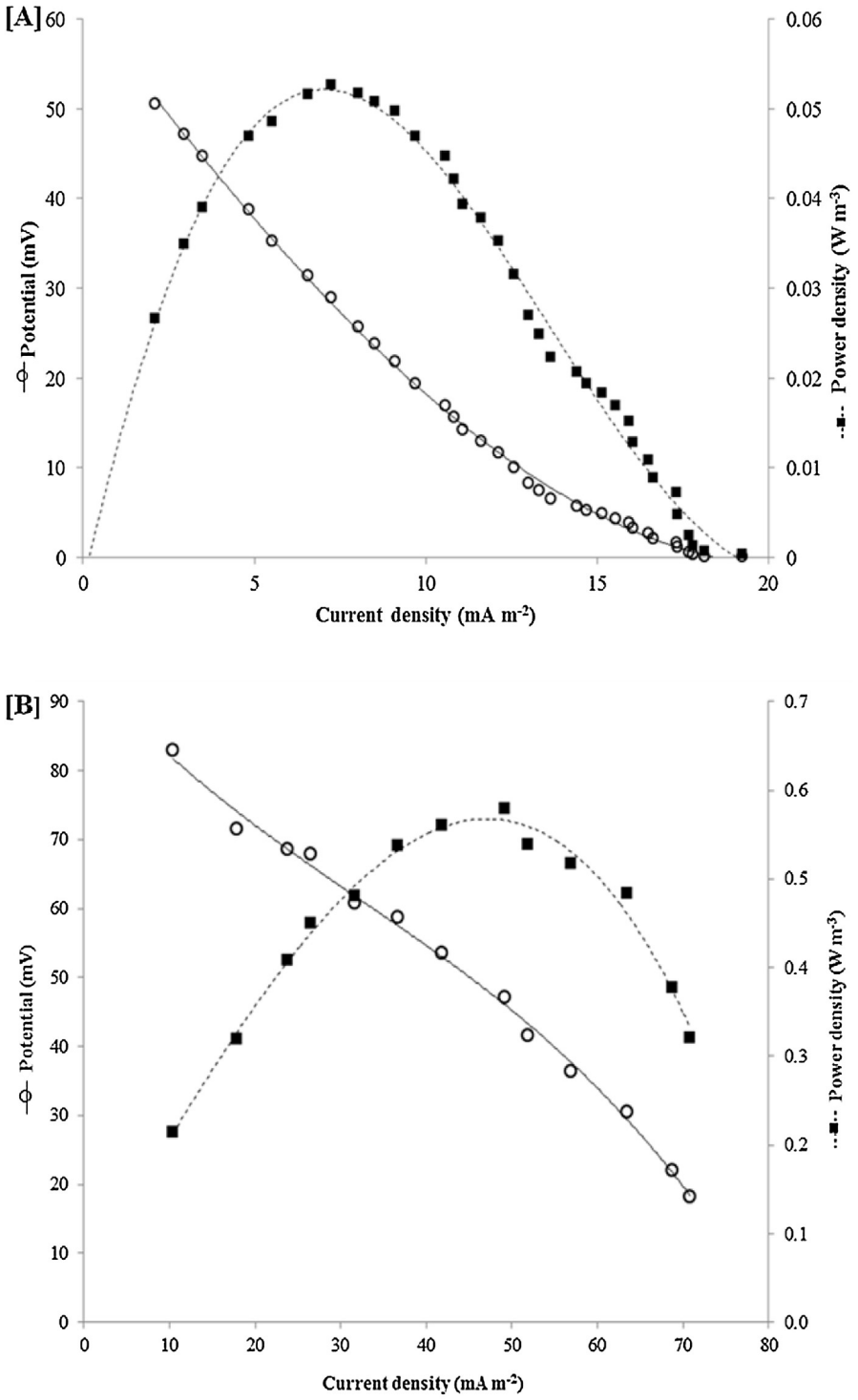

Fig. 3. Power and polarisation curves. A: MFC_S; B: MFC_L. Current density refers to the anode surface area: MFC_S = 16 mm^2; MFC_L = 32 mm^2. Volumetric power density refers to the MFC chamber volume: MFC_S = 64 μL; MFC_L = 128 μL. For each geometry, data is the average of 3 devices, with up to 22% error.

The internal resistance (R_{int}) of the MFC was calculated from the linear fit of the ohmic region of each polarisation cell potential curve ($R_{int} = \Delta V/\Delta I$), as previously described [3].

2.5. Stacking

To scale-up the power output, MFC units with the same geometry were electrically stacked in series and in parallel, as shown in Fig. 2. The MFCs were enriched individually and stacked after the five days of enrichment, once a steady current was generated. Once stacked, the MFC units were fed in parallel with AUM and no bacteria. The polarisation experiments on the stack were performed after at least 24 hours of operation.

2.6. Calculations

The maximum current density (I_{max}) under mass transport limiting conditions at the electrode, is expressed according to [27] as:

$$I_{max} = nFD\frac{\Delta C}{\lambda} \quad (1)$$

Where n is number of electrons equivalent corresponding to the limiting compound (substrate), F is Faraday's constant (96485C mol^{-1}), D is the normalised diffusivity of the limiting compound (substrate) ($m^2\,s^{-1}$), ΔC is the concentration gradient of the limiting compound ($mol\,m^{-3}$), and λ is the diffusion layer thickness (m).

The Reynold's number (Re) and mass transfer coefficient (k_C) for laminar flow in a channel is defined as [28]:

$$Re = \frac{\rho v d_H}{\mu} \quad (2)$$

$$k_c = 0.664(Re)^{1/2}\left(\frac{\mu}{\rho D}\right)^{1/3}\left(\frac{D}{H}\right) \quad (3)$$

Where ρ is specific density of the fluid ($kg\,m^{-3}$), v is the linear velocity of the fluid ($m\,s^{-1}$), d_H is the hydraulic diameter of the flow channel (m), and μ is the viscosity of the fluid ($kg\,m^{-1}\,s^{-1}$).

The hydraulic diameter of the channel (d_H) is related to the channel length according to Equation 4:

$$d_H = \frac{4(LH)}{2(L+H)} \quad (4)$$

Where H is the height (m), and L is the lateral dimension length (m).

The diffusion-layer thickness (λ) at the electrode surface was calculated with the following equation:

$$\lambda = \frac{D}{k_c} \quad (5)$$

3. Results and Discussion

3.1. Effect of Electrode Length on Performance

The influence of the electrode length on the performance of small scale MFCs, was investigated in this study by operating two different fuel cells geometries, MFC_S and MFC_L, characterised by the same cross sectional area (and therefore the same electrode spacing, 4 mm) but different channel lengths. In particular, the length of the anodic chamber in MFC_L was two times larger than MFC_S. The resulting performances are compared in terms of the power and cell polarisation curves, produced from the polarisation experiment, as shown in Fig. 3.

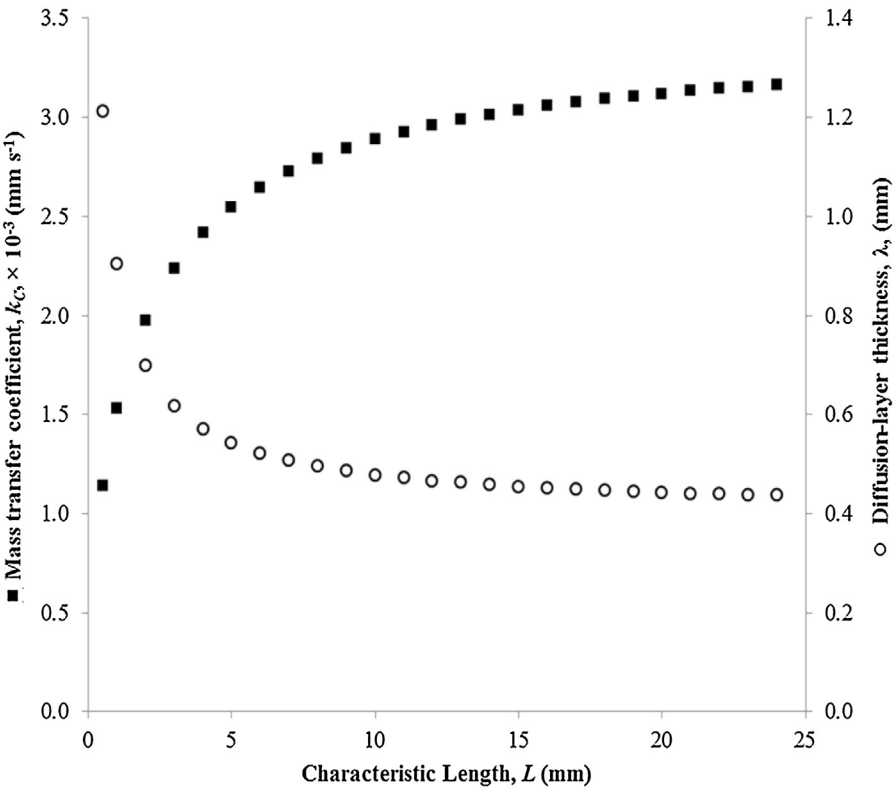

Fig. 4. Effect of length of MFC channel on mass transfer coefficient and diffusion-layer thickness moving from 0.5 to 25 mm. Values plotted are for a flow rate of 0.36 mL min^{-1}.

The OCV for MFC_S and MFC_L were 253 ± 86 mV and 312 ± 59 mV respectively. High internal resistances were observed for both devices. In particular, MFC_L showed an internal resistance of 33 kΩ, which is comparable to the values of miniature MFCs reported in the literature [29,30]. The internal resistance of MFC_S was higher at 242 kΩ. From the cell polarisation curves in Fig. 3, ohmic losses appear to be dominating in both MFC_S and MFC_L, suggesting that the electrical resistances of the electrodes, membrane and electrolyte are mostly responsible for the internal resistance of the MFC. Accordingly, there is little evidence of mass transfer limitations taking place in the MFC, which may be a result of miniaturisation, which, as expected, allows good transfer of substrate from the bulk fluid to the biofilm on the anode [31].

Doubling the length of the anode chamber improved the power density by a factor of 11. The maximum power densities of MFC_S and MFC_L were 0.053 and 0.580 W m^{-3} respectively, and the current densities at the maximum power output were 7.3 and 49.1 mA m^{-2} respectively.

The increase in power and current density is suspected to be due to an increase in the mass transfer between the bulk fluid, biofilm and electrode surface. When observing the cross section of a MFC square electrode chamber, the height, *H*, and the lateral dimension (length), *L*, will affect the performance of the device. On one hand, when the height of the channel is reduced (i.e. the distance between electrodes is reduced) in the MFC, the miniaturised device benefits from a greater rate of mass transfer due to an increase in the surface area to volume ratio of the device [23]. As a result, the power density generated by miniature MFCs is

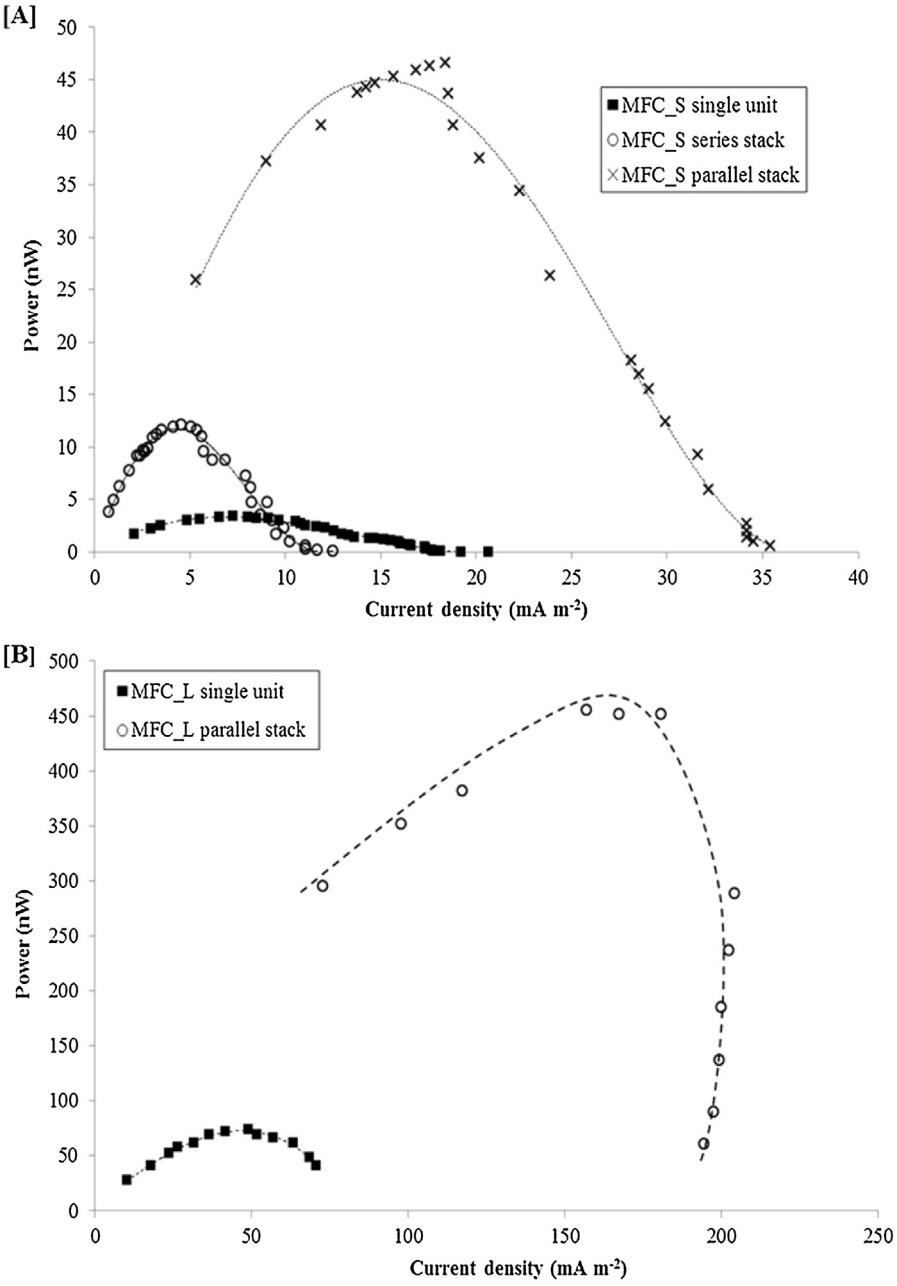

Fig. 5. Power and polarisation curves. A) Refers to MFC_S, operated alone, in series and in a parallel stack. Current density refers to the anode surface area, 16 mm^2 for a single unit, 48 mm^2 for the stack. B) Refers to MFC_L, operated alone and in a parallel stack. Current density refers to the anode surface area, 32 mm^2 for a single unit, 96 mm^2 for the stack.

higher than large-scale devices [32]. On the other hand, when the lateral dimension of the channel (length), *L*, of the electrode chamber is increased, the hydraulic diameter of the channel is increased as per Equation 4. Consequently, the mass transfer coefficient, k_C, will increase as per Equations 2 and 3. Therefore, when *L* is increased, whilst maintaining a fixed *H*, the mass transfer coefficient is increased, and hence the diffusion-layer thickness at the electrode surface will decrease (Equation 5). By altering the length of the channel, the maximum current density available at the electrode will therefore increase (Equation 1), and, consequently, result in high fuel consumption efficiency and an improvement in power performance.

Fig. 4 demonstrates that increasing the length of the flow channel, for a fixed flow rate, will increase the mass transfer coefficient and decrease the diffusion-layer thickness. Values here have been calculated using Equations 1–5, with the flow rate at 0.36 mL min^{-1}, and a linear velocity of 22.5 mm min^{-1}. For urine, the kinematic viscosity (μ/ρ) is estimated to be 1.07 mm^2 s^{-1} at 20 °C [33], and the diffusivity of urea in water is 0.082 mm^2 min^{-1} [34].

To ensure that these assumptions are valid, the flow regime in the flow channel must be laminar. This is confirmed by the *Re* values for MFC_S and MFC_L, which are 1.4 and 1.9 respectively, as calculated by considering *L* values of 4 and 8 mm, for MFC_S and MFC_L respectively, and *H* equal to 4 mm.

By increasing the length of the electrode in the MFC devices, a better fuel efficiency has been achieved, with consequent improvement in performance [35]. This is in accordance with a recent study by [36] whereby increasing the length of a graphite fibre brush anode from 12 mm to 30 mm the power density increased from 1.13 to 1.65 W m^{-2}. The better supply of redox species (c) to the anode leads to an increase in the measured current density (I), according to equation 6:

$$I = nF\frac{K_c}{\lambda}c \quad (6)$$

Where: n is the moles of electrons involved in the reaction; F (C mol^{-1}) is the Faraday constant; K_c (m s^{-1}) is the mass transfer coefficient; λ (m) is the diffusion layer thickness; c is the concentration of the redox compound (mol m^{-3}).

3.2. Stacking the Miniature MFCs

To scale up the power output, MFC_S and MFC_L were arranged in stacks of three units each. The MFC_S units were electrically connected either in parallel or in series to evaluate the best configuration.

Fig. 5A reports the results from the polarisation experiments. The maximum power output increased almost 4 times when the MFC_S units operated as a series stack compared to individual units, while when stacked in parallel the power output was 14 times higher. This result is in agreement with previous studies that report voltage reversal effects when the MFCs are arranged in series [37]. The reversal in some of the cells in the series stack is caused by the unavoidable increase in the internal resistances of the MFC units operated in series, as previously reported [37,38]. Thereby, power performance is reduced. When operated in parallel however, if the impedances of the MFCs are well matched, then the internal resistance of the MFC stack will tend towards the lowest common denominator and thus be more uniform [39]. This is evident by the reduction in internal resistance of the MFC_S stack from 244 to 76 kΩ. This large reduction in the internal resistance may also explain the increase in the current density of the parallel stack from 7.3 mA m^{-2} to 18.4 mA m^{-2}, as summarised in Table 1.

Considering the results obtained for the MFC_S stacks, the MFC_L devices were arranged only in parallel. As shown in Fig. 5B, in this case the maximum power output of the stack was nearly 6 times higher compared to the MFC_L individual units. The power density increased by a factor of 2, and the internal resistance decreased from 33 kΩ to 1.4 kΩ (Table 1).

The stacking of larger MFCs (mL scale) has been shown to increase the power density of MFCs, albeit not to the extent observed in this report. For example power densities of millilitre scale MFCs (6.25 and 12 mL) were improved by a factor of 1.2-1.4 by stacking multiple units together [9,38]. On the other hand, Aelterman et al. [40] demonstrates similar power densities between individual units and MFC stacks when using 60 mL MFCs.

3.3. Use of Biomass-Derived ORR Catalysts

To enhance power generation, without compromising cost-effectiveness and sustainability, two biomass-derived carbon materials, BC1 and BC2, were tested as ORR catalysts at the cathode. Since MFC_L showed better performance, this study was carried out only on this fuel cell design. The resulting fuel cells were named as MFC_BC1 and MFC_BC2 according to the type of catalyst used. Table 1 summarises the results obtained and compares them with the catalyst-free fuel cells previously tested. Fig. 6 shows the polarisation and power curves for both devices. The OCV values for MFC_BC1 and MFC_BC2 were 151 mV and 220 mV respectively, and thus comparable with MFC_L.

As expected, the ORR catalysts enhanced the power performance of the MFCs, leading to a power output and power density almost 3 times higher than MFC_L. The effectiveness of biomass-derived ORR catalysts may be attributed to the large surface area [19] that the materials exhibit on the cathode surface compared to the plain carbon cloth (BC1: 376 m^2 g^{-1}), as well as the capacity of heteroatom doping, such as nitrogen and sulphur, or the incorporation of nanoparticles like iron within the catalyst material to enhance the ORR activity [17,18,41–44].

The internal resistances decreased to values of 15 kΩ and 23 kΩ, for MFC_BC1 and MFC_BC2 respectively, down to half those of MFC_L. Consequently, the current densities were an order of magnitude higher, with a value as high as 127.6 mA m^{-2} for MFC_BC1.

Table 1
Summary of performance of the several MFCs tested in this study.

MFC configuration	OCV (mV)	Internal resistance (kΩ)	Maximum power output (nW)	Maximum volumetric power density (W m^{-3})	Maximum current density (mA m^{-2})
MFC_S	253	242	3.4	0.053	7.3
MFC_S series stack	151	243	12.1	0.063	4.6
MFC_S parallel stack	206	76	46.7	0.243	18.4
MFC_L	312	33	74.2	0.580	49.1
MFC_L parallel stack	281	1.4	455.1	1.185	157.1
MFC_BC1	151	15	250.1	1.954	127.6
MFC_BC2	220	23	220.1	1.719	88.4

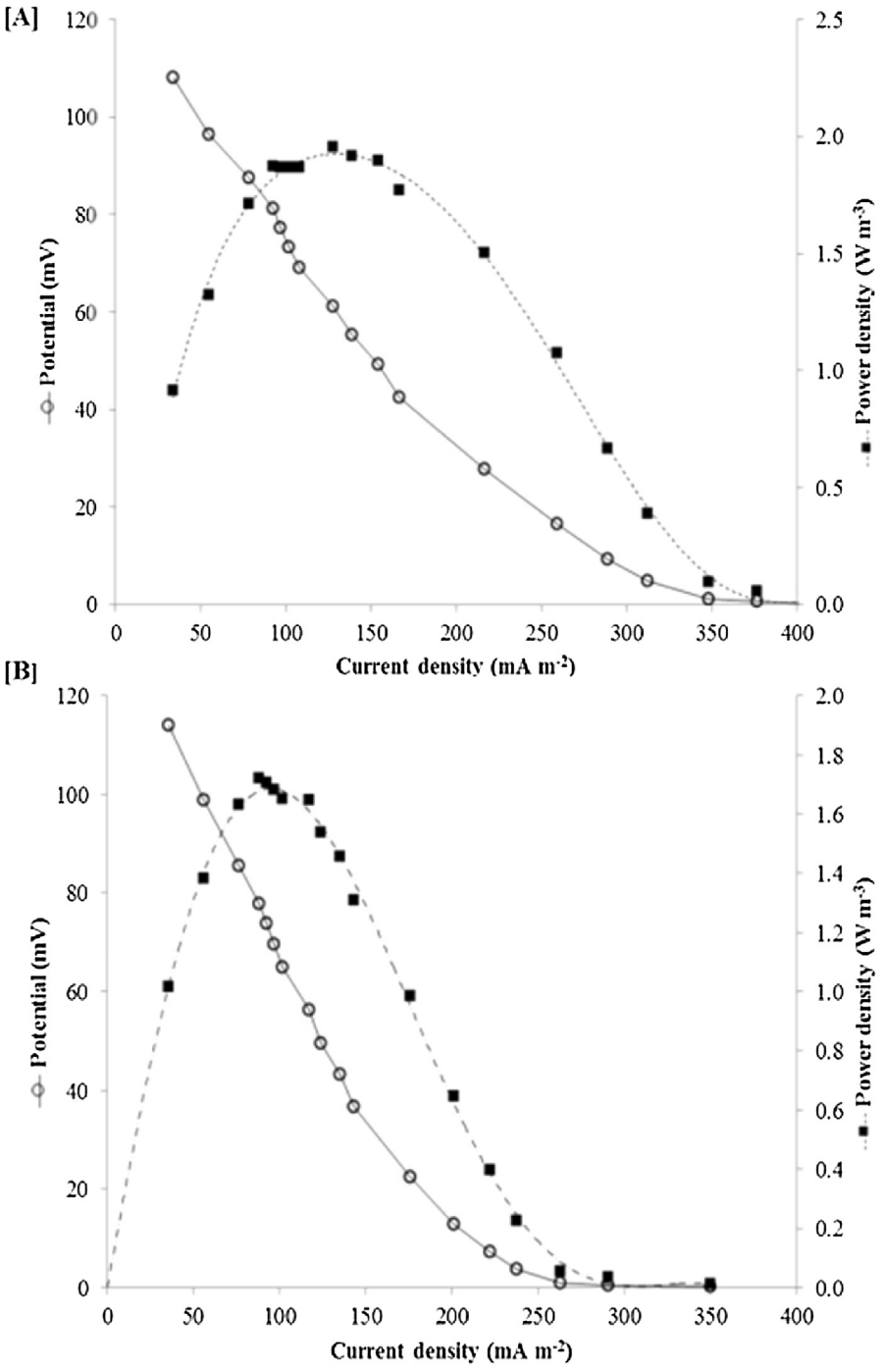

Fig. 6. Power and polarisation curves. A) refers to MFC_BC1; B) refers to MFC_BC2; Current density refers to the anode surface area: MFC_BC1, MFC_BC2 = 32 mm^2. Volumetric power density refers to the MFC chamber volume: MFC_BC1, MFC_BC2 = 128 μL. MFC_BC1 is data from one device, and MFC_BC2 is an average of two units with 17% error.

Generally MFC_BC1 performed better, with a 13% higher power density and a 44% increase in current density, compared to MFC_BC2. The structure of the two doped cathodes may be the reason for this difference. From the SEM images of the doped cathodes (Fig. 7), it can be seen that the two ORR catalysts led to very different surface structures. In particular, it appears that BC1 percolated between the carbon fibres of the carbon cloth. Hence, good contact was formed between the carbon fibre electrode and the biomass-derived ORR catalyst, thus allowing a good active surface area for oxygen reduction reactions at the cathode surface. On the other hand, BC2 formed a porous layer on top of the carbon fibres, which have resulted in an added resistance to the system and may explain the poorer performance of MFC_BC2 with respect to MFC_BC1.

4. Conclusions

Microbial fuel cells are an extremely attractive technology for the generation of clean electricity from a range of waste streams. The most viable route to boosting power density generated by

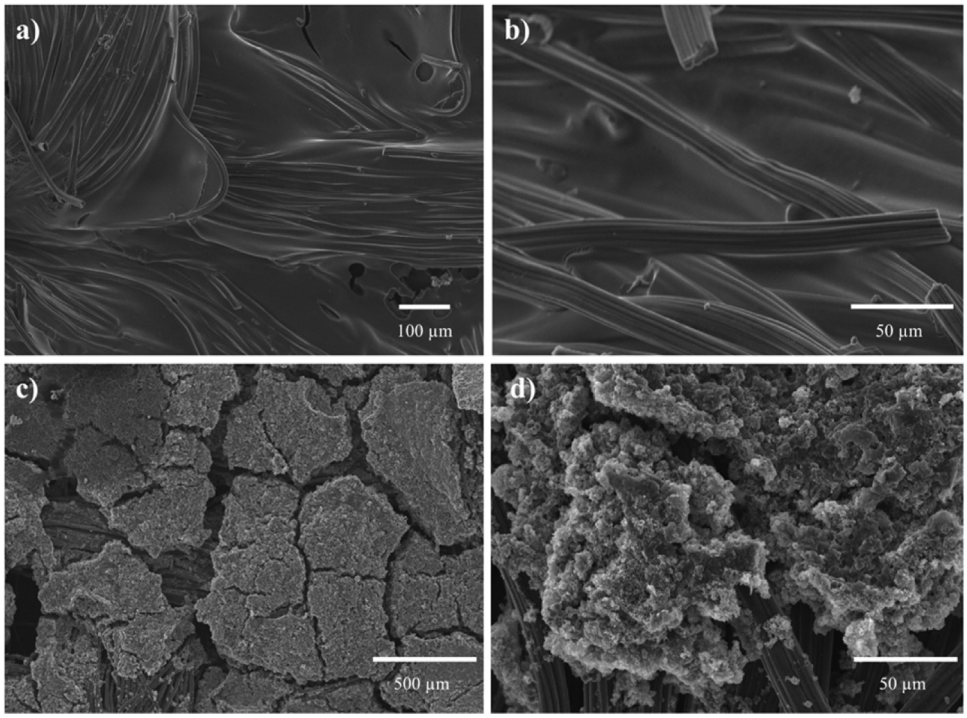

Fig. 7. SEM images of the two biomass-derived ORR catalyst doped cathode surfaces. a) and b) refer to the cathode used for MFC_BC1; c) and d) to the case of MFC_BC2.

MFCs is to develop small scale devices and arrange multiple units in stacks.

In this context, our study aims to guide towards the development of effective miniature MFCs. For this purpose we have developed an innovative miniature MFC, which can easily be further miniaturised. We have used an air-cathode configuration since it has the advantage of greater operational simplicity and cost-effectiveness. While fixing the electrodes spacing to 4 mm, we have investigated the effect of the electrodes length, when the system was continuously fed with artificial urine at a fixed flow rate of 0.36 mL min^{-1}.

The doubling of the electrode length of the miniature MFC, and so the hydraulic retention time as well, increased the power density more than tenfold due to enhanced mass transfer properties and substrate consumption at the electrode surface.

By electrically stacking three individual units in parallel, the power output reached the peak value of 1.2 W m^{-3}. Moreover, the use of two different types of biomass-derived ORR catalysts at the cathode increased the power density up to threefold. These renewable and cost-effective cathode catalysts are of particular interest for applications in remote or impoverished regions where MFCs could be used for remote and sustainable energy generation from waste.

Acknowledgements

The authors thank: Wessex Water for providing anaerobic sludge; the Engineering and Physical Sciences Research Council (EPSRC) and the Doctoral Training Centre for Sustainable Chemical Technologies (CSCT) for funding (EP/K014889/1); Stephen Bradley for the SEM images of the doped cathodes. Ioannis Ieropoulos is an EPSRC career acceleration fellow (CAF), grant numbers EP/I004653/1 and EP/L002132/1.

References

[1] O. Edenhofer, R. Pichs-Madruga, Y. Sokona, K. Seyboth, P. Matschoss, S. Kadnert, Renewable Energy Sources and Climate Change Mitigation- Special Report of the Intergovernmental Panel on Climate Change, 2011.
[2] A.P.C. Faaij, Bio-energy in Europe: changing technology choices, Energy Policy 34 (2006) 322–342, doi:http://dx.doi.org/10.1016/j.enpol.2004.03.026.
[3] B. Logan, U. Rozendal, J. Keller, S. Freguia, et al., Critical Review Microbial Fuel Cells : Methodology and Technology, Environ. Sci. Technol. 40 (2006) 5181–5192.
[4] I. Ieropoulos, J. Greenman, C. Melhuish, Urine utilisation by microbial fuel cells; energy fuel for the future, Phys. Chem. Chem. Phys. 14 (2012) 94–98, doi:http://dx.doi.org/10.1039/c1cp23213d.
[5] H. Ren, H.-S. Lee, J. Chae, Miniaturizing microbial fuel cells for potential portable power sources: promises and challenges, Microfluid. Nanofluidics. 13 (2012) 353–381, doi:http://dx.doi.org/10.1007/s10404-012-0986-7.
[6] K. Rabaey, W. Verstraete, Microbial fuel cells: novel biotechnology for energy generation, Trends Biotechnol. 23 (2005) 291–298, doi:http://dx.doi.org/10.1016/j.tibtech.2005.04.008.
[7] H. Liu, B.E. Logan, Electricity generation using an air-cathode single chamber microbial fuel cell in the presence and absence of a proton exchange membrane, Environ. Sci. Technol. 38 (2004) 4040–4046. http://www.ncbi.nlm.nih.gov/pubmed/15298217.
[8] I. Ieropoulos, P. Ledezma, A. Stinchcombe, G. Papaharalabos, C. Melhuish, J. Greenman, Waste to real energy: the first MFC powered mobile phone, Phys. Chem. Chem. Phys. 15 (2013) 15312–15316, doi:http://dx.doi.org/10.1039/c3cp52889h.
[9] I. Ieropoulos, J. Greenman, C. Melhuish, Miniature microbial fuel cells and stacks for urine utilisation, Int. J. Hydrogen Energy. 38 (2013) 492–496, doi:http://dx.doi.org/10.1016/j.ijhydene.2012.09.062.
[10] Z. He, J. Kan, Y. Wang, Y. Huang, F. Mansfeld, K.H. Nealson, Electricity Production Coupled to Ammonium in a Microbial Fuel Cell, Environ. Sci. Technol. 43 (2009) 3391–3397, doi:http://dx.doi.org/10.1021/es803492c.
[11] S. Choi, Microscale microbial fuel cells: Advances and challenges, Biosens. Bioelectron. 69 (2015) 8–25, doi:http://dx.doi.org/10.1016/j.bios.2015.02.021.
[12] I. Baudler, A. Langner, U. Schröder, Does it have to be Carbon? Metal Anodes in Microbial Fuel Cells and related Bioelectrochemical Systems, Energy Environ. Sci. (2015), doi:http://dx.doi.org/10.1039/C5EE00866B.
[13] B. Logan, J. Regan, Microbial challenges and applications, Environ. Sci. Technol. 40 (2006) 5172–5180, doi:http://dx.doi.org/10.1021/es0627592.
[14] L. Deng, M. Zhou, C. Liu, L. Liu, C. Liu, S. Dong, Development of high performance of Co/Fe/N/CNT nanocatalyst for oxygen reduction in microbial fuel cells, Talanta 81 (2010) 444–448, doi:http://dx.doi.org/10.1016/j.talanta.2009.12.022.

[15] L. Zhang, C. Liu, L. Zhuang, W. Li, S. Zhou, J. Zhang, Manganese dioxide as an alternative cathodic catalyst to platinum in microbial fuel cells, Biosens. Bioelectron. 24 (2009) 2825–2829, doi:http://dx.doi.org/10.1016/j.bios.2009.02.010.
[16] T. Huggins, H. Wang, J. Kearns, P. Jenkins, Z.J. Ren, Biochar as a sustainable electrode material for electricity production in microbial fuel cells, Bioresour. Technol. 157 (2014) 114–119, doi:http://dx.doi.org/10.1016/j.biortech.2014.01.058.
[17] Y. Yuan, T. Yuan, D. Wang, J. Tang, S. Zhou, Sewage sludge biochar as an efficient catalyst for oxygen reduction reaction in an microbial fuel cell, Bioresour. Technol. 144 (2013) 115–120, doi:http://dx.doi.org/10.1016/j.biortech.2013.06.075.
[18] H. Yuan, L. Deng, Y. Qi, N. Kobayashi, J. Tang, Nonactivated and Activated Biochar Derived from Bananas as Alternative Cathode Catalyst in Microbial Fuel Cells, Sci. World J. 2014 (2014).
[19] S.-A. Wohlgemuth, R.J. White, M.-G. Willinger, M.-M. Titirici, M. Antonietti, A one-pot hydrothermal synthesis of sulfur and nitrogen doped carbon aerogels with enhanced electrocatalytic activity in the oxygen reduction reaction, Green Chem. 14 (2012) 1515, doi:http://dx.doi.org/10.1039/c2gc35309a.
[20] M. Li, Y. Xiong, X. Liu, C. Han, Y. Zhang, X. Bo, et al., Iron and nitrogen co-doped carbon nanotube@hollow carbon fibers derived from plant biomass as efficient catalysts for the oxygen reduction reaction, J. Mater. Chem. A 3 (2015) 9658–9667, doi:http://dx.doi.org/10.1039/C5TA00958H.
[21] T.H. Pham, K. Rabaey, P. Aelterman, P. Clauwaert, L. De Schamphelaire, N. Boon, et al., Microbial Fuel Cells in Relation to Conventional Anaerobic Digestion Technology, Eng. Life Sci. 6 (2006) 285–292, doi:http://dx.doi.org/10.1002/elsc.200620121.
[22] L. Woodward, M. Perrier, B. Srinivasan, C. Hc, B. Tartakovsky, Maximizing Power Production in a Stack of Microbial Fuel Cells Using Multiunit Optimization Method, Biotechnol. Prog. 25 (2009) 676–682, doi:http://dx.doi.org/10.1021/bp.115.
[23] F. Qian, D.E. Morse, Miniaturizing microbial fuel cells, Trends Biotechnol. 29 (2011) 62–69, doi:http://dx.doi.org/10.1016/j.tibtech.2010.10.003.
[24] F. Qian, Z. He, M.P. Thelen, Y. Li, A microfluidic microbial fuel cell fabricated by soft lithography, Bioresour. Technol. 102 (2011) 5836–5840, doi:http://dx.doi.org/10.1016/j.biortech.2011.02.095.
[25] T. Brooks, C.W. Keevil, A simple artificial urine for the growth of urinary pathogens, Lett. Appl. Microbiol. 24 (1997) 203–206. http://www.ncbi.nlm.nih.gov/pubmed/9080700.
[26] R.J. White, N. Yoshizawa, M. Antonietti, M.-M. Titirici, A sustainable synthesis of nitrogen-doped carbon aerogels, Green Chem. 13 (2428) (2011), doi:http://dx.doi.org/10.1039/c1gc15349h.
[27] C.I. Torres, P. Parameswaran, B.E. Rittmann, J. Chae, Improved current and power density with a micro-scale microbial fuel cell due to a small characteristic length, Biosens. Bioelectron. 61 (2014) 587–592, doi:http://dx.doi.org/10.1016/j.bios.2014.05.037.
[28] T.K. Sherwood, R.L. Pigford, C.R. Wilke, Mass Transfer, McGraw-Hill, New York, 1975.
[29] S. Choi, Y. Yang, P. Parameswaran, C.I. Torres, B.E. Rittmann, et al., A μL-scale micromachined microbial fuel cell having high power density, Lab Chip. 11 (2011) 1110–1117, doi:http://dx.doi.org/10.1039/c0lc00494d.
[30] F. Qian, M. Baum, Q. Gu, D.E. Morse, A 1.5 microL microbial fuel cell for on-chip bioelectricity generation, Lab Chip. 9 (2009) 3076–3081, doi:http://dx.doi.org/10.1039/b910586g.
[31] A. Elmekawy, H.M. Hegab, X. Dominguez-Benetton, D. Pant, Internal resistance of microfluidic microbial fuel cell: challenges and potential opportunities, Bioresour. Technol. 142 (2013) 672–682, doi:http://dx.doi.org/10.1016/j.biortech.2013.05.061.
[32] A. Wang, C.-Y. Huang, D.-J. Lee, J.-S. Chang, Micro-sized microbial fuel cell: a mini-review, Bioresour. Technol. 102 (2011) 235–243, doi:http://dx.doi.org/10.1016/j.biortech.2010.07.007.
[33] B. Inman, W. Etienne, R. Rubin, R. Owusu, T. Oliveira, D. Rodriques, et al., The impact of temperature and urinary constituents on urine viscosity and its relevance to bladder hyperthermia treatment, Int. J. Hyperth. 29 (2013) 206–210, doi:http://dx.doi.org/10.3109/02656736.2013.775355.
[34] B.Y. Louis, D. Akeley, A Study of the Diffusion of Urea in Water at 25C with the Gouy Interference Method, J. Am. Chem. Soc. 74 (1952) 2058–2060, doi:http://dx.doi.org/10.1021/ja01128a060.
[35] J. Lee, K.G. Lim, G.T.R. Palmore, A. Tripathi, Optimization of microfluidic fuel cells using transport principles, Anal. Chem. 79 (2007) 7301–7307, doi:http://dx.doi.org/10.1021/ac070812e.
[36] C. Liu, J. Li, X. Zhu, L. Zhang, D. Ye, R.K. Brown, et al., Effects of brush lengths and fiber loadings on the performance of microbial fuel cells using graphite fiber brush anodes, Int. J. Hydrogen Energy. 38 (2013) 15646–15652, doi:http://dx.doi.org/10.1016/j.ijhydene.2013.03.144.
[37] I. Ieropoulos, J. Greenman, C. Melhuish, Improved energy output levels from small-scale Microbial Fuel Cells, Bioelectrochemistry 78 (2010) 44–50, doi:http://dx.doi.org/10.1016/j.bioelechem.2009.05.009.
[38] P. Ledezma, J. Greenman, I. Ieropoulos, MFC-cascade stacks maximise COD reduction and avoid voltage reversal under adverse conditions, Bioresour. Technol. 134 (2013) 158–165, doi:http://dx.doi.org/10.1016/j.biortech.2013.01.119.
[39] G. Papaharalabos, J. Greenman, C. Melhuish, I. Ieropoulos, A novel small scale Microbial Fuel Cell design for increased electricity generation and waste water treatment, Int. J. Hydrogen Energy. 40 (2015) 4263–4268, doi:http://dx.doi.org/10.1016/j.ijhydene.2015.01.117.
[40] P. Aelterman, K. Rabaey, H.T. Pham, N. Boon, W. Verstraete, Continuous Electricity Generation at High Voltages and Currents Using Stacked Microbial Fuel Cells, Environ. Sci. Technol. 40 (2006) 3388–3394, doi:http://dx.doi.org/10.1021/es0525511.
[41] J. Liu, P. Song, Z. Ning, W. Xu, Recent Advances in Heteroatom-Doped Metal-Free Electrocatalysts for Highly Efficient Oxygen Reduction Reaction, Electrocatalysis. 6 (2015) 132–147, doi:http://dx.doi.org/10.1007/s12678-014-0243-9.
[42] N. Daems, X. Sheng, I.F.J. Vankelecom, P.P. Pescarmona, Metal-free doped carbon materials as electrocatalysts for the oxygen reduction reaction, J. Mater. Chem. A. 2 (2014) 4085–4110, doi:http://dx.doi.org/10.1039/C3TA14043A.
[43] F. Charreteur, F. Jaouen, S. Ruggeri, J.-P. Dodelet, Fe/N/C non-precious catalysts for PEM fuel cells: Influence of the structural parameters of pristine commercial carbon blacks on their activity for oxygen reduction, Electrochim. Acta. 53 (2008) 2925–2938, doi:http://dx.doi.org/10.1016/j.electacta.2007.11.002.
[44] J. Kramm, T.M. Larouche, M. Lefèvre, F. Jaouen, et al., Structure of the catalytic sites in Fe/N/C-catalysts for O_2-reduction in PEM fuel cells, Phys. Chem. Chem. Phys. 14 (2012) 11673–11688, doi:http://dx.doi.org/10.1039/c2cp41957b.